

PRACTICAL APPROACH TO MODELING OF WOOD TRUSS ROOF ASSEMBLIES

By Zhong Li,¹ Rakesh Gupta,² and Thomas H. Miller³

ABSTRACT: The main objective of this study was to investigate a practical approach to model trusses and roof truss systems using a commercially available software program, ETABS. The model developed in this study takes into account the system behavior from load sharing and composite action, the semirigidity of the metal-plate-connected joints, and joint eccentricity. The model was verified by comparing the predicted deflections, member internal forces, truss strengths, and load sharing of roof systems with the full-scale experimental results available in the literature.

INTRODUCTION

Metal-plate-connected (MPC) trusses are widely used in light-frame construction as the main vertical load-carrying elements in roof and floor systems. These trusses have traditionally been designed based on a tributary load distribution. The current design method ignores connection semirigidity and joint eccentricity in MPC trusses, load distribution by roof sheathing from timber trusses to stiffer trusses, partial composite action that exists between the top-chord member and the sheathing, as well as the variability in the correlated stiffness and strength properties of the truss wood members. The inclusion of these factors could improve the design of MPC trusses resulting in savings of natural resources. The objective of this study was to include joint semirigidity and eccentricity in truss model and load sharing and composite action in a roof truss assemblies model by using a commercially available software used by practicing engineers.

The long-term goals of this project are to investigate the system performance of MPC wood truss assemblies and determine strength increase factors for wood members used in truss construction. This paper describes the first step in the research and demonstrates the applicability of a commercial structural analysis program to investigate the system behavior of truss assemblies.

LITERATURE REVIEW

There is strong evidence of load sharing in wood truss roof systems. Full-scale roof truss assembly tests at the Forest Products Laboratory (FPL) in Madison, Wisconsin, revealed that 35–66% of the applied load was distributed to the unloaded trusses when one truss was loaded individually in truss roof assemblies (Wolfe and McCarthy 1989; Wolfe and LaBissoniere 1991). The interactions between the sheathing material and truss members, as well as the high variability in stiffness of the wood members, contribute to the strength increase of a truss system. A wood truss system actually performs better than expected using the current design method. Therefore, it is of practical importance to find the system effect in wood roof truss assemblies.

Wolfe et al. (1986) tested full-scale individual trusses and found that trusses have linear deflection performance up to twice the design load and only slight deviations from linearity up to three times the design load. King and Wheat (1987) also found that load-deflection and load-member axial force curves for nine MPC, parallel-chord trusses were linear up to the design load.

Cramer and Wolfe (1989) developed a three-dimensional frame analysis program (ROOFSYS) to model a roof system of trusses connected by plywood sheathing. Plywood sheathing on each side of a pitched roof system was represented by a single continuous beam having bending stiffnesses about two axes. Nail slip between the sheathing beam and the truss top chords was assumed to have a negligible effect on system performance and was ignored. The T-beam effect of the attached sheathing was accounted for by using the bending stiffness equation developed for the deflection of a simply supported, partially composite T-beam by Kuenzi and Wilkinson (1971). Although no attempt was made to include connector plate semirigidity, it was found that this model reasonably predicted assembly load distributions.

LaFave and Itani (1992) developed a roof assembly model by assigning rotational and uniaxial fixity factors to the MPC wood members that provided a better prediction of roof assembly behavior. The developed model did not require experimentally derived connector plate parameters.

Perhaps the most comprehensive model for the analysis of load sharing and composite action is NARSYS (nonlinear analysis of roof systems) developed by Mtenga (1991). This model provided a reasonable prediction of the stiffnesses and strengths of individual trusses outside of an assembly, but load sharing for a truss assembly was not verified.

TRUSS AND TRUSS SYSTEM MODELS

In this study truss and truss assemblies were modeled using a widely available commercial software program, ETABS (Computers and Structures, Inc., Berkeley, Calif.) This software is used by practicing engineers to analyze a variety of structures. Some of the techniques in modeling truss and truss assemblies were obtained from the available literature as discussed later.

MPC Fink trusses and truss systems were modeled with two main types of elements: beam elements and spring elements. Wood truss and plywood sheathing members were modeled using beam elements. The heel joints and bottom-chord-tension-splice joints were modeled using ETABS spring elements. The spring elements have no physical dimensions and were used to represent semirigid behavior at the ends of wood truss members connected by metal plates, which are modeled by "rigid" links. Fig. 1 shows the semirigid truss model using ETABS for a 3:12 slope, MPC roof truss.

The truss system model included nine trusses connected by sheathing beams. The plywood sheathing itself was treated as

¹Engr. Systems Analyst, Tee-Lok Corp, Edenton, N.C. 27932; formerly, Grad. Res. Asst., Dept. of Forest Products and Civ., Constr. and Envir. Engrg., Oregon State Univ., Corvallis, OR 97331.

²Assoc. Prof., Dept. of Forest Products, Oregon State Univ., Corvallis, OR.

³Assoc. Prof., Dept. of Civ., Constr. and Envir. Engrg., Oregon State Univ., Corvallis, OR.

Note. Discussion open until January 1, 1999. To extend the closing date one month, a written request must be filed with the ASCE Manager of Journals. The manuscript for this paper was submitted for review and possible publication on October, 1997. This paper is part of the *Practice Periodical on Structural Design and Construction*, Vol. 3, No. 3, August, 1998. ©ASCE, ISSN 1084-0680/98/0003-0119-0124/\$8.00 + \$.50 per page. Paper No. 16795.

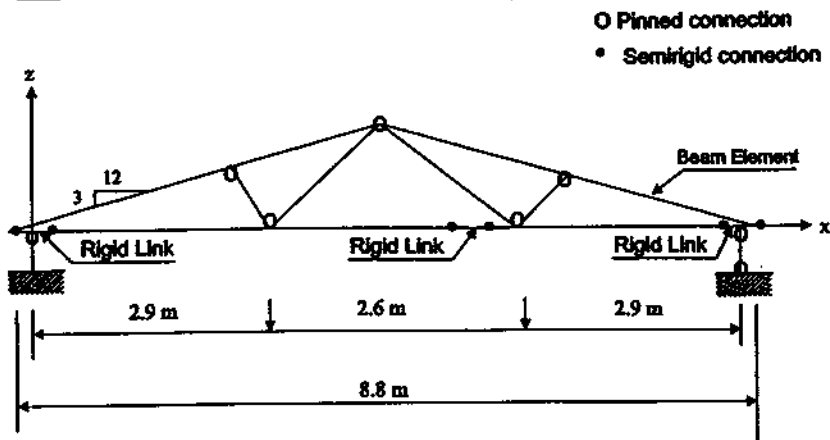


FIG. 1. Semirigid Truss Model Using ETABS

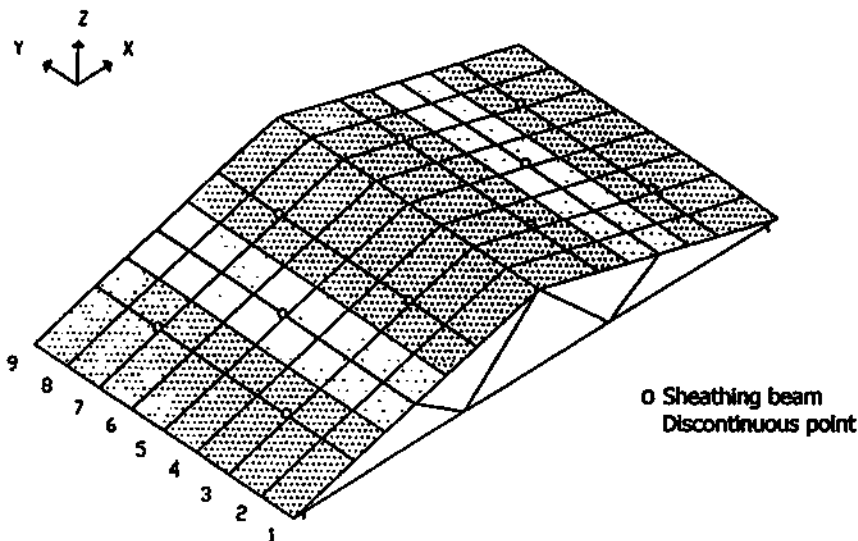


FIG. 2. Truss System Model Using ETABS

a deep beam with one of the principal axes aligned with the top chord members of the trusses and the other principal axis perpendicular to the plywood sheathing plane. In the truss system model, plywood sheathing was divided into three sheathing beam elements on each side by tributary areas and these sheathing beam elements have the same thickness as the plywood sheathing (Fig. 2). Therefore, there are six sheathing beam elements in the truss system model. The truss beam elements are rectangular with cross sections the same as the wood members and are aligned with the centroidal axes of the members.

Spring Elements

Each plate-wood contact area for the MPC heel joints and bottom-chord-tension-splice joints was modeled by a set of three zero-length springs representing two axial stiffnesses and one rotational stiffness. The stiffnesses of these springs were derived based on experimental load-slip characteristics of MPC connections, assuming that each tooth contributes equally to the stiffnesses and the rotational spring stiffness of each plate-wood contact area is dependent on the corresponding translational spring stiffnesses. For simplification, the non-linear behavior of the MPC joints was assumed to be linear and modeled using ETABS linear spring elements. The ETABS spring element has six input stiffnesses. In the two-dimensional analysis conducted for individual trusses, one of the three axial stiffnesses and two of the three rotational stiffnesses (out of the truss plane) were set to infinity.

Spring stiffnesses of each plate-wood contact area for heel joints and bottom-chord-tension-splice joints were functions of the plate-wood contact area, the tooth density of the metal plate, and the experimentally determined stiffnesses of the plate tooth-wood connection. There are two plate-wood contact areas at each heel joint and tension-splice joint. Each contact area was modeled by an ETABS spring element. Therefore, to include semirigidities of two heel joints and one tension-splice joint, six spring elements were used in the semirigid truss model. The locations of the spring elements were arbitrarily placed near the center of each plate-wood contact area. For convenience in ETABS input, the spring element for the plate-wood contact area at the top chord of the heel joint was assumed to be located at the intersection between center lines of the truss top chord and bottom chord. The spring element for the plate-wood contact area at the bottom chord of the heel joint was assumed to be located at the intersection between the vertical center of gravity line of the plate-wood contact area at the bottom chord and the horizontal center line of the bottom chord member. The spring elements for the plate-wood contact area of the tension-splice joint were assumed to be located at the center of gravity of each plate-wood contact area. A spring element for a plate-wood contact area was connected to the spring element for the other plate-wood contact area from the same metal plate through a rigid link. A rigid link was assumed to have the same dimensions as the truss wood member with a modulus-of-elasticity value the same as steel.

Foschi (1977) developed a model to relate MPC joint stiff-

nesses to plate orientation with respect to grain direction of the wood members and the load direction. Use of Foschi's model requires the determination of the three parameters to fit the experimental load-displacement curves for four standard joint configurations. Foschi's parameters for any other cases can be obtained by using a Hankinson-type interpolation (Foschi 1977). For directions along the plate major axis (axis 1) and plate minor axis (axis 2), the Foschi parameters are

$$k_1 = \frac{k_{AA}k_{AE}}{k_{AA} \sin^2\Phi + k_{AE} \cos^2\Phi} \quad (1)$$

and

$$k_2 = \frac{k_{EE}k_{AE}}{k_{EE} \sin^2\Phi + k_{EA} \cos^2\Phi} \quad (2)$$

Here k_1 and k_2 are any one of Foschi's parameters at orientations parallel to the plate major axis and minor axis, respectively; k_{AA} , k_{AE} , k_{EA} , and k_{EE} are Foschi's parameters for the four standard joint configurations; and Φ is the angle between the plate major axis and the grain direction. Because metal plates were placed horizontally with the plate major axis (axis 1) in the horizontal direction and the plate minor axis (axis 2) in the vertical direction, spring stiffnesses along these two axes were used as axial stiffnesses of the ETABS spring elements (which only allow vertical or horizontal axial stiffness input).

Although (1) and (2) apply to all of Foschi's parameters, here only the initial stiffness k is used to determine spring stiffnesses because of the linear model used in this study. The spring stiffnesses K of a metal plate-wood contact area in the horizontal (x -axis) and vertical (z -axis) directions can be expressed as functions of the stiffness of a single tooth (Mtenga 1991)

$$K_x = k_x \cdot A \cdot \beta \quad (3)$$

$$K_z = k_z \cdot A \cdot \beta \quad (4)$$

The rotational spring stiffness of a metal plate-wood contact area can be derived from the two translational spring stiffnesses as (Mtenga 1991)

$$K_{rotation} = \beta \cdot (k_x \cdot I_x + k_z \cdot I_z) \quad (5)$$

where k_x , k_z = Foschi parameters for the initial stiffnesses of a single tooth along the horizontal (x -axis) and the vertical (z -axis) directions; K_x , K_z = translational spring stiffnesses for a plate-wood contact area along the horizontal (x -axis) and the vertical (z -axis) directions; A = plate-wood contact area; β = tooth density of the metal plate; and I_x , I_z = moments of inertia of plate-wood contact area.

From these equations, the stiffnesses of the spring element at heel joints and tension-splice joints were calculated (Li 1997).

Top Chord Elements

The bending stiffnesses of truss top chord members were increased to take into account the partial composite action between the plywood sheathing and top chord members. Kuenzi and Wilkinson (1971) developed an equation relating the deflections of a partially composite beam with that of a completely composite beam. In this method, the deflection of a partially composite T-beam for a floor joist (web of T-beam) nailed with sheathing (flange of T-beam) is given by

$$\Delta = \Delta_r \left[1 + f_\Delta \left(\frac{EI_r}{EI_u} - 1 \right) \right] \quad (6)$$

where Δ = deflection of the partially composite beam; Δ_r = deflection of the completely composite beam (the components

of the beam are rigidly connected); $f_\Delta = 10/(L^2\alpha^2 + 10)$; L = beam span; α = functions of h , s , EI_r , EI_u ; h = distance between the centroidal axes of the flange and web; s = load per unit length, which causes a unit slip in the nail; EI_r = bending stiffness if the components are rigidly connected; and EI_u = bending stiffness if the components are completely unconnected.

The effective stiffness, EI , of a partially composite beam can be expressed in terms of EI_u and EI_r . Noting that $\Delta/\Delta_r = EI_r/EI$, (6) can be rewritten as (Kuenzi and Wilkinson 1971)

$$EI = \frac{EI_u}{EI_u(1 - f_\Delta)/EI_r + f_\Delta} \quad (7)$$

In roof truss assemblies, the truss top chords function as partially composite beams and the increased bending stiffnesses of truss top chords can be approximately determined using (7).

Sheathing Beam Elements

Not only does the plywood sheathing contribute to an increase in the stiffnesses of truss top chord members due to partial composite action, but it also functions as a distributor beam to transfer the load from loaded or stiffer trusses to unloaded or more limber trusses. The plywood sheathing in this project was modeled by sheathing beam elements, which are three-dimensional beam elements having six degrees of freedom at each end and are connected to the top chord member of each truss in the assembly. The gaps in the plywood sheathing were taken into account by discontinuing (using a pin joint) those sheathing beams at the trusses that approximately correspond to the gap locations. Fig. 2 shows the continuity of sheathing beams in a truss system model.

Joint Eccentricity

When there are more than two truss members connected through a MPC at a truss joint, the center lines of the members usually do not intersect at one point. This causes an eccentricity at the joint. Eccentricity occurs in the heel joints and web joints, as well as in the ridge joints in the pitched Fink trusses. If these connections are simplified as common nodes that join wood elements together, the eccentricities are ignored. This simplification may lead to errors in analyzing the structure. The input of eccentric joints in ETABS is complicated; therefore, for practical consideration only, the eccentricity of the heel joint was modeled in this project. At the heel joint, the intersection point between the top chord and bottom chord members is offset some distance along the bottom chord from the intersection point between the center line of the truss bearing plate and truss bottom chord. This was modeled by adopting one node for each intersection point at the heel connection (Fig. 1). Also, two very short column elements representing the truss bearing plates were used in the model. The locations of these columns were the same as the center lines of the truss bearing plates. These columns have very large out-of-truss plane stiffnesses. Within the truss plane, one of the column elements is very rigid to represent the pin connection at one end of the truss. The other column element is very flexible to represent the roller connection at the other end of the truss.

RESULTS AND DISCUSSIONS

Model Verification

Next, the semirigid truss and nine-truss roof system models were verified by comparing the predicted deflections, member internal forces, truss strengths, and load-sharing of four nine-

truss roof systems with the experimental results. Member internal forces for Fink trusses were not available from the literature; therefore, member internal force verification was conducted through comparisons between the predicted and the tested member internal forces for parallel-chord trusses tested by King and Wheat (1987).

Deflection and Member Internal Force Verification

Deflection comparisons were made between experimental and predicted deflections from the semirigid models. Twenty-four residential roof trusses with Fink configurations of 3:12 and 6:12 slope tested at the FPL (Wolfe et al. 1986) were used for this purpose. These 8.5-m-span trusses were constructed in three stiffness categories of low, medium, and high modulus of elasticity (MOE) values. Fig. 3 shows the deflection comparisons when these trusses are subjected to a uniform load of 800 N/m for 3:12 trusses and 960 N/m for 6:12 trusses along the truss top chords. These deflections are the average values measured at the five truss node points (four web joints and one crown joint). As shown in Fig. 3, most of the predicted average deflections are within 7% of the test results.

King and Wheat (1987) tested nine MPC parallel-chord wood trusses with three different configurations (three trusses for each configuration). All trusses were designed using nominal 38 mm × 89 mm lumber with 20-gauge metal plates and were loaded uniformly to the design load of 1,170 N/m along the top chords. Detailed notes and measurements were made on all trusses and truss deflections along the bottom chords and member internal forces were recorded. The ETABS semirigid model for these parallel chord trusses is shown in Fig. 4 (all dimensions are along the web center lines of truss members). The semirigidities of all MPC connections are included and each plate-wood contact area is modeled with an ETABS spring element located at the intersection between the web center line and the horizontal center of the gravity line of the plate-wood contact area. The sizes of metal plates in actual trusses range from 76 × 76 mm to 152 × 102 mm and an average size of 102 × 102 mm was used to calculate the stiff-

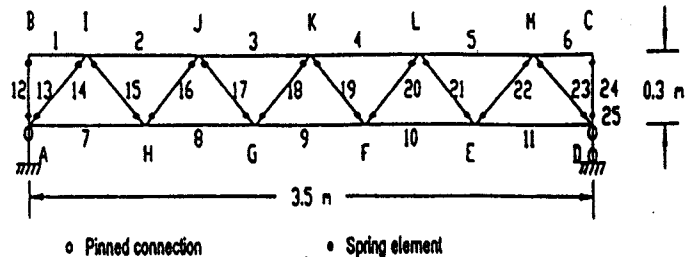


FIG. 4. ETABS Semirigid Model of Parallel Chord Truss Tested by King and Wheat (1987)

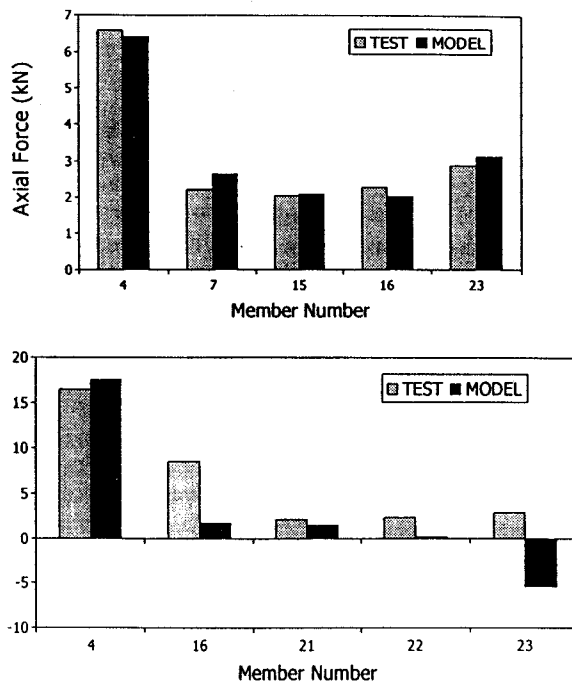


FIG. 5. Axial Force and Bending Moment Comparisons for Parallel Chord Trusses Tested by King and Wheat (1987)

nesses. Member axial forces and member bending moments from tested results, Wheat's analog 4 model using fictitious members, and the ETABS semirigid model for one truss are compared in Fig. 5. The other comparisons are given by Li (1997). The comparisons show that for axial forces most predicted values are within 10% of the test results, but for bending moments, larger differences are observed for some members. It is also clear from Fig. 5 that the ETABS model predicts axial forces close to the experimentally obtained axial forces and the ETABS model predicted nonzero bending moments reasonably well in the web members.

Strength Verification

To determine strengths of trusses and truss assemblies, it is essential to have an understanding of the relationship between strengths and stiffnesses of truss wood members and the failure criteria for different loading conditions.

The strength-MOE relationships given by Gerhards (1983) were used in determining the strength of wood members. The following failure criteria for wood members were used in this study.

For combined bending and axial tension

$$f_c/ITS + f_b/BS > 1.0 \quad (8)$$

For combined bending and axial compression

$$(f_c/CS)^2 + f_b/BS > 1.0 \quad (9)$$

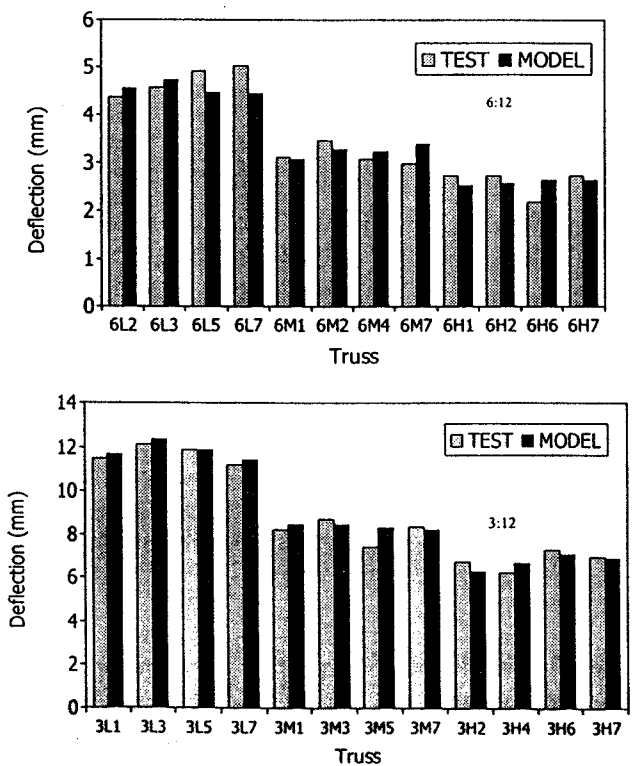


FIG. 3. Deflection Comparison for 3:12 and 6:12 Trusses Tested by Wolfe et al. (1986)

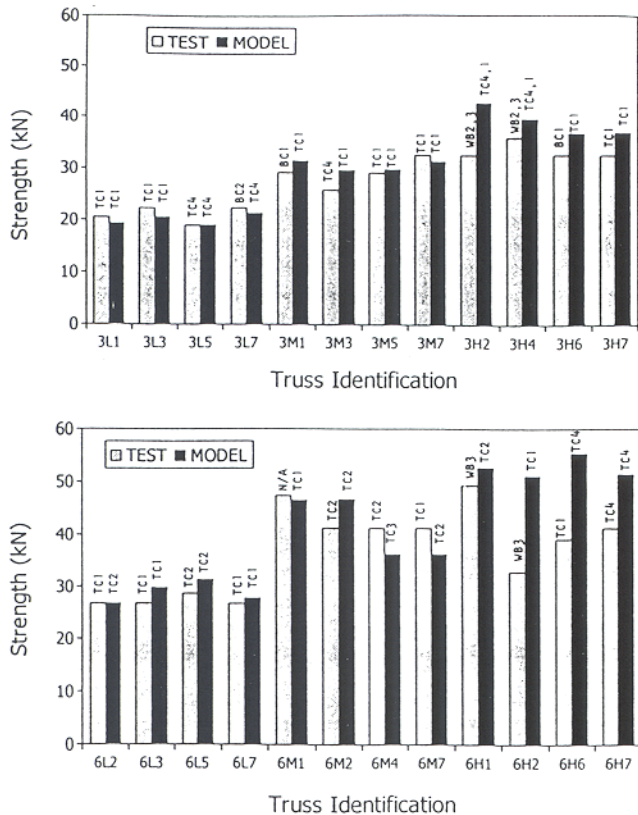


FIG. 6. Strength Comparisons for Trusses Tested by Wolfe et al. (1986)

where f_t , f_b , and f_c = tensile, bending, and compressive stresses in members, respectively; and TS , BS , and CS = tensile, bending, and compressive strengths of members, respectively. Although Fink truss tests at the FPL (Wolfe and LaBissoniere 1991) revealed that Fink trusses mostly failed at the heel joints, joint failures in this study are considered at heel joints, tension-splice joints and web joints at bottom chords. The failure criteria for these joints are

$$P > P_{\text{failure}} \quad (10)$$

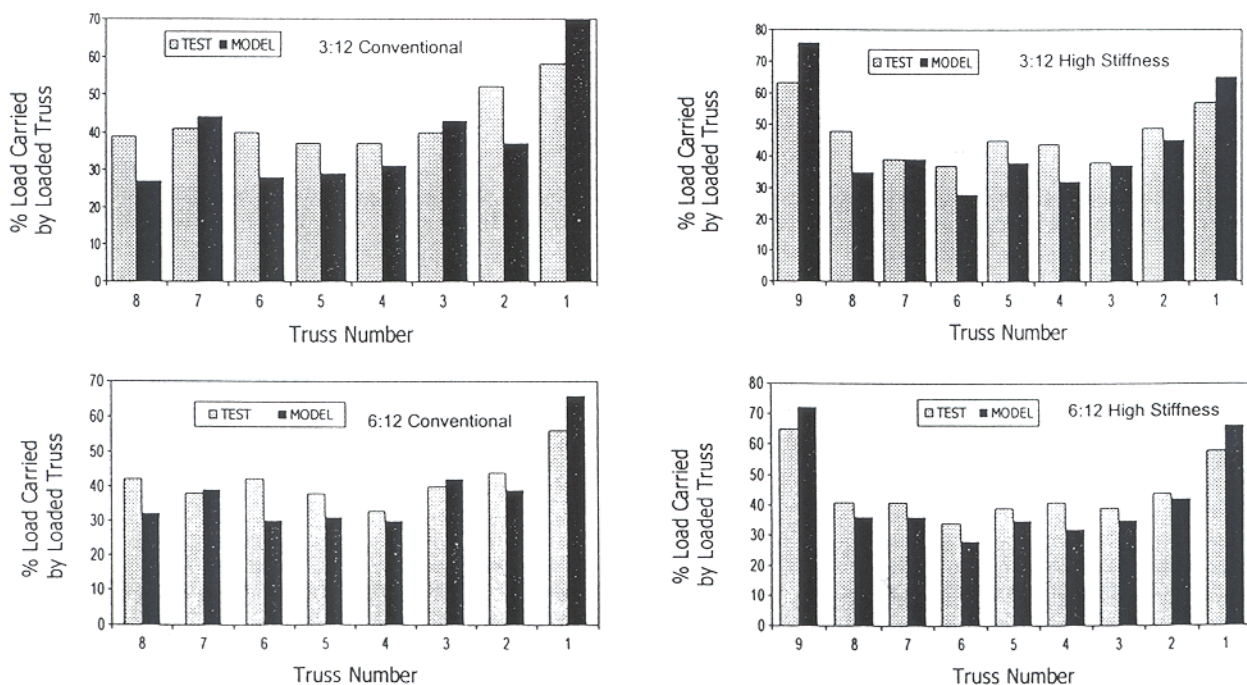


FIG. 7. Load-Sharing Comparisons for Assemblies Tested by Wolfe and McCarthy (1989) and Wolfe and LaBissoniere (1991)

where the P values are the axial compressive force in the top chord of the heel joint, the bottom chord tensile force for the tension splice joint, and the web tensile force in the tension member of the web at the bottom chord joint. P_{failure} values are the corresponding failure loads for these joints. The failure loads (P_{failure}) for these joints were taken from Gupta (1990), who tested 56 heel joints, 52 tension-splice joints, and 55 web joints at the bottom chords.

The strengths for 24 trusses tested outside of roof assemblies are compared with the strengths predicted by the semi-rigid model. These trusses were made from southern pine no. 2 and tested at the FPL by Wolfe et al. (1986). The failed member in each tested truss is also compared with the predicted failed member from the truss model. Joint failure is not considered in the strength modeling of these trusses, because these trusses were overplated at heel joints and tension-splice joints with 16-gauge plates and strength data for 16-gauge MPC joints were not available from the literature. Fig. 6 shows the strength and failed member comparisons where the term "model" refers to the semirigid model used in this study. Truss strength predicted by the ETABS model is generally within 9% of the tested strength and the model almost always predicted the correct member failure.

Load-Sharing Verification

Load-sharing results from two series of full-scale roof truss assemblies tested at the FPL by Wolfe and McCarthy (1989) and Wolfe and LaBissoniere (1991) were used for comparison with load-sharing predicted by the truss system model. These two series are truss assemblies with high stiffness variability and truss assemblies with low stiffness variability as for conventional construction. Each series included two truss assemblies, one with a 3:12 slope and the other with a 6:12 slope. In the truss assemblies with low stiffness variability, one of the previously failed trusses tested outside the assembly was sheathed with plywood and used as an exterior truss (truss 9) in the assemblies. Each truss in the assembly was loaded uniformly one at a time, except for the exterior truss made of the failed truss. The vertical reaction forces at the supports were recorded. Load-sharing was found by dividing the sum of the vertical reactions for each truss by the total applied load. This

gives the load distributed to each truss when one of the trusses is loaded in the roof assembly. Modulus of elasticity for each wood truss member used in the FPL assembly tests was used in the truss system model. The experimental and predicted load sharing are shown in Fig. 7, where the terms Test and Model refer to the tested and predicted results, respectively. The MOE values for wood members in the exterior failed truss were arbitrarily increased five times to model the very rigid truss sheathed with plywood.

Each bar in these figures shows the load carried by the truss when it alone is loaded in the truss assembly. Comparisons of load carried by the other trusses in the assemblies are given by Li (1997). Comparing the predicted with the experimental load sharing, the maximum percentage difference for load distributed to the loaded trusses is 15% for 3:12 slope truss assemblies with an average value of 8%, and 10% for 6:12 slope truss assemblies with an average value of 6%. For more realistic loading, where all trusses are loaded in the assembly at the same time, the predicted load distribution is very close to the tested load distribution. For example, when all trusses in the 3:12 slope truss assembly with high stiffness variability were loaded, the test load carried by the middle truss is 13%, whereas the predicted load carried by the middle truss is 15%.

CONCLUSIONS

Computer models for MPC trusses and truss assemblies were developed using a commercially available software, ETABS. Model verification includes deflection, truss member internal force, truss strength, and load-sharing comparisons of predicted with experimental results, and showed that a commercially available structural analysis software can be used to investigate the system behavior of truss assemblies. It also shows the potential application of a commercially available program used by practicing engineers to model and design roof

systems. Thus, truss system design may be improved by including system behavior directly, rather than using system modification factors to design single trusses.

APPENDIX. REFERENCES

- Cramer, S. M., and Wolfe, R. W. (1989). "Load-distribution model for light-frame wood roof assemblies." *J. Struct. Engrg.*, ASCE, 115(10), 2602-2617.
- Foschi, R. O. (1977). "Analysis of wood diaphragms and trusses. Part II: Truss-plate connections." *Can. J. Civ. Engrg.*, 4, 353-362.
- Gerhards, C. C. (1983). "Characterization of physical and mechanical properties of 2 by 4 truss lumber." *Res. Paper FPL-431*, U.S. Department of Agriculture, Forest Products Laboratory, Madison, Wis.
- Gupta, R. (1990). "Reliability analysis of semirigidly connected metal plate residential wood trusses," PhD dissertation, Cornell University, Ithaca, N.Y.
- King, C. G., and Wheat, D. L. (1987). "Deflection and member behavior of metal-plate connected parallel-chord wood trusses." *Res. Rep.*, Dept. of Civ. Engrg., University of Texas, Austin, Tex.
- Kuenzi, E. W., and Wilkinson, T. L. (1971). Composite beams—effect of adhesive or fastener rigidity. *Res. Paper FPL-152*, U.S. Department of Agriculture, Forest Products Laboratory, Madison, Wis.
- LaFave, K., and Itani, R. (1992). "Comprehensive load distribution model for wood truss assemblies." *Wood and Fiber Sci.*, 24(1), 79-88.
- Li, Z. (1997). "A practical approach to model the behavior of a metal-plate-connected wood truss system," MS thesis, Oregon State University, Corvallis, Oreg.
- Mtenga, P. V. (1991). "Reliability of light-frame wood roof systems," PhD thesis, University of Wisconsin, Madison, Wis.
- Wolfe, R. W., Percival, D. H., and Moody, R. C. (1986). "Strength and stiffness of light-framed sloped trusses." *Res. Paper FPL 471*, Forest Products Laboratory, Madison, Wis.
- Wolfe, R. W., and McCarthy, M. (1989). "Structural performance of light-frame roof assemblies—I. Truss assemblies designed for high variability and wood failure." *Res. Paper FPL-RP-492*, U.S. Department of Agriculture, Forest Products Laboratory, Madison, Wis.
- Wolfe, R. W., and LaBissoniere, T. (1991). "Structural performance of light-frame roof assemblies—II. Conventional truss assemblies." *Res. Paper FPL-RP-499*, U.S. Department of Agriculture, Forest Products Laboratory, Madison, Wis.